

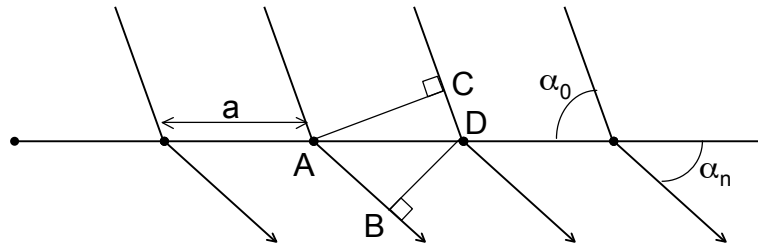
Theory of data collection

- Diffraction geometry,
- The rotation method,
- Beam and crystal parameters
- Integration

Harry Powell

A useful discussion of diffraction of light and of X-rays is in Christopher Hammond's book "The Basics of Crystallography and Diffraction" (particularly chapters 7 and 8 in the 2nd edition); while it may be rather old-fashioned in its style, it deals with the basics of Laue and Bragg diffraction and the Ewald sphere construction in a clear and logical way. For those who are less interested in the mathematics (and written in a more readable style), David Blow's "Outline of Crystallography for Biologists" is recommended.

Scattering from a one-dimensional crystal

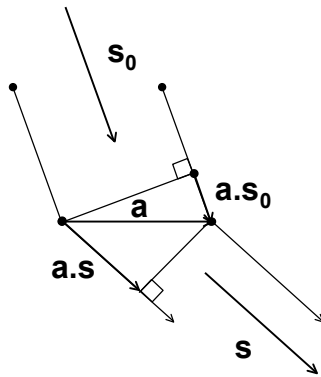


only get constructive interference if

$$AB - CD = n\lambda$$
$$= a (\cos\alpha_n - \cos\alpha_0)$$

(First Laue equation)

The path difference between the individual beams must be an integral number of wavelengths for constructive interference. All other situations will result in the X-rays being “cancelled out” over their path through the crystal.



first Laue equation expressed in vector notation

$$a (\cos\alpha_n - \cos\alpha_0) = \mathbf{a} \cdot (\mathbf{s} - \mathbf{s}_0)$$

\mathbf{s} , \mathbf{s}_0 are unit vectors

Extend this to three dimensions to give the three Laue equations:

$$a (\cos\alpha_n - \cos\alpha_0) = \mathbf{a} \cdot (\mathbf{s} - \mathbf{s}_0) = n_x \lambda$$

$$b (\cos\beta_n - \cos\beta_0) = \mathbf{b} \cdot (\mathbf{s} - \mathbf{s}_0) = n_y \lambda$$

$$c (\cos\gamma_n - \cos\gamma_0) = \mathbf{c} \cdot (\mathbf{s} - \mathbf{s}_0) = n_z \lambda$$

for constructive interference from a three dimensional lattice all three equations must be satisfied simultaneously
i.e.

6 angles - $\alpha_n, \alpha_0, \beta_n, \beta_0, \gamma_n, \gamma_0$

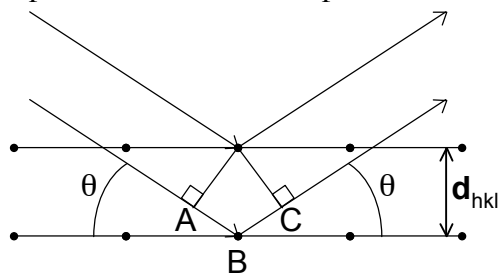
3 lattice lengths - a, b, c

3 integers - $n_x \lambda, n_y \lambda, n_z \lambda$

Plainly, dealing with 12 variables for each reflection is something of a handful; this appears to be the main reason why the Laue equations are rarely referred to directly, and a simpler representation is used instead. The reflecting conditions can be described by the Bragg equation, or can be envisioned using the Ewald sphere construction.

Bragg's alternative analysis

W.L Bragg (the son, see photo by stairwell by the TMV model) noticed that diffraction spots on X-ray photographs have the appearance of specular reflections of "pencil-beams" of light

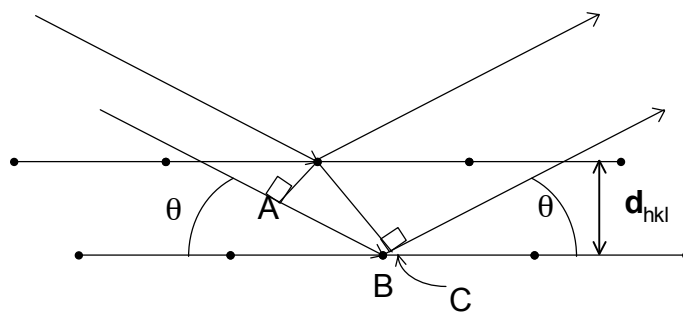


for constructive interference:

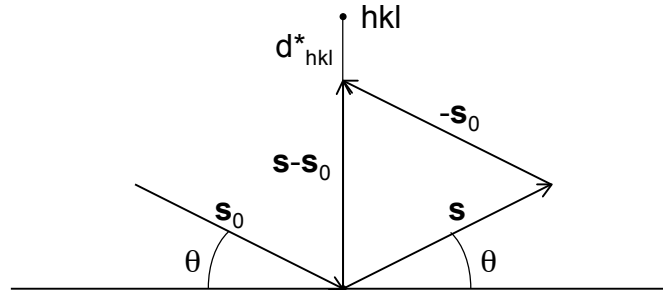
$$\begin{aligned} AB + BC &= d_{hkl} \sin\theta + d_{hkl} \sin\theta \\ &= 2d_{hkl} \sin\theta \\ &= n\lambda \end{aligned}$$

Note

- (1) this construction has rather fewer variables than the Laue equations because reflections are wholly represented in two dimensions
- (2) It also works for the general case where $AB \neq BC$, i.e. we can treat it as reflection from reciprocal lattice planes rather than scattering from atoms.



Bragg's Law in vector notation; the reciprocal lattice



$$|\mathbf{s} - \mathbf{s}_0| = 2\sin\theta$$

$$|\mathbf{d}^*_{hkl}| = 1/d_{hkl}$$

$$(\mathbf{s} - \mathbf{s}_0)/\lambda = \mathbf{d}^*_{hkl} = h\mathbf{a}^* + k\mathbf{b}^* + l\mathbf{c}^*$$

Hence constructive interference only occurs when $(\mathbf{s} - \mathbf{s}_0)/\lambda = \mathbf{d}^*_{hkl}$.

This formulation can be combined with each of the three Laue equations, *e.g.*

$$\mathbf{a} \cdot (\mathbf{s} - \mathbf{s}_0) = n_x \lambda$$

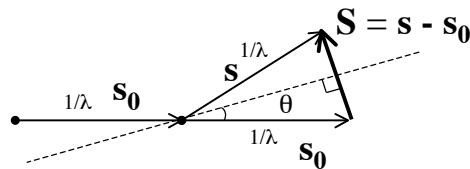
$$= \mathbf{a} \cdot \mathbf{d}^*_{hkl} \cdot \lambda$$

$$= \mathbf{a} \cdot (h\mathbf{a}^* + k\mathbf{b}^* + l\mathbf{c}^*) \lambda$$

hence

$$n_x = h \text{ (since } \mathbf{a} \cdot \mathbf{a}^* = 1, \mathbf{a} \cdot \mathbf{b}^* = 0, \mathbf{a} \cdot \mathbf{c}^* = 0)$$

The Ewald Sphere Construction

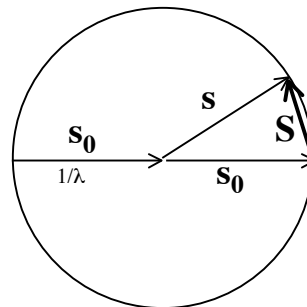


The general condition for diffraction is illustrated by the vector equation $\mathbf{S} = \mathbf{s} - \mathbf{s}_0$

Because \mathbf{s}_0 and \mathbf{s} have the same length ($1/\lambda$), we can generalise this diagram by drawing a sphere of radius $|\mathbf{s}_0| = |\mathbf{s}| = 1/\lambda$

\mathbf{S} is the diffraction vector in *reciprocal space*

For a crystal, \mathbf{S} may only take certain values, $\mathbf{S} = h \mathbf{a}^* + k \mathbf{b}^* + l \mathbf{c}^*$



The diffraction vector \mathbf{S} corresponds to the distance between planes in reciprocal space, usually represented as d_{hkl}^* . The representation here is preferred by Jan Drenth in “Principles of Protein Crystallography”; his treatment may be preferred to that of Hammond.

Diffraction of the beam represented by the vector \mathbf{s}_0 giving the vector \mathbf{s} may be thought of as reflection from the dotted line in the top diagram (as in Bragg’s Law).

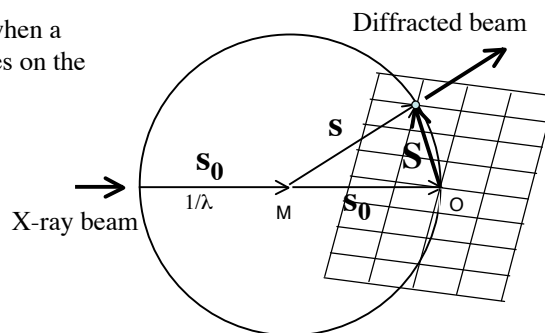
The Ewald sphere is only a construction but is very useful to understand the *geometry* of diffraction. Confusingly, it has *two* origins:-

M is the centre of the sphere, and may be considered as the position of the crystal, since this is the source of the secondary beam s

O is the origin of reciprocal space, the origin of the diffraction vector S , and the centre of the reciprocal lattice

As the crystal rotates, the reciprocal lattice rotates in exactly the same way

Diffraction only occurs when a reciprocal lattice point lies on the sphere

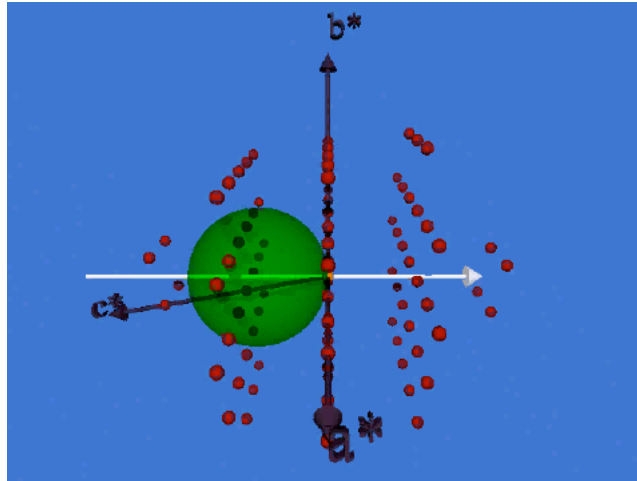


It may be useful to think of the crystal at the centre of the Ewald sphere being linked to the centre (origin) of the reciprocal lattice by something like a bicycle chain - the two “objects” rotate exactly in step with each other.

The origin of the reciprocal lattice corresponds to the (0,0,0) reflection - *i.e.* the direct beam.

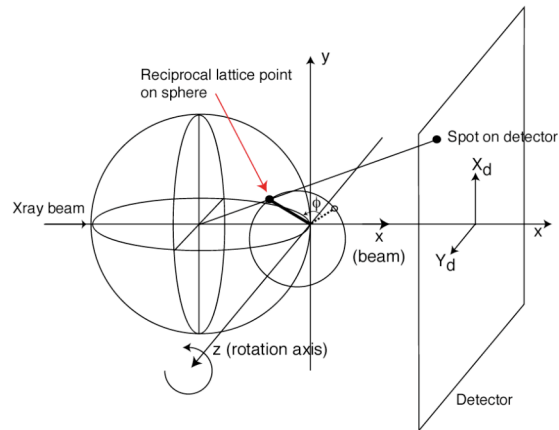
As the crystal rotates, so does the the reciprocal lattice

As a reciprocal lattice point passes through the Ewald sphere, a diffracted beam is observed along the line from the sphere centre to the reciprocal lattice point



<http://www-sphys.unil.ch/x-ray>

The part of the reciprocal lattice which intersects the sphere is projected on to the detector

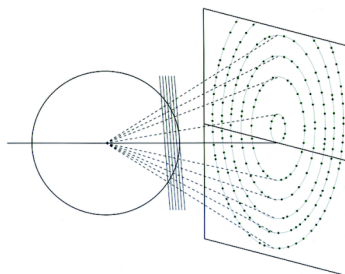


As the crystal rotates, each lattice point in turn passes through the sphere, and a spot is recorded on the detector

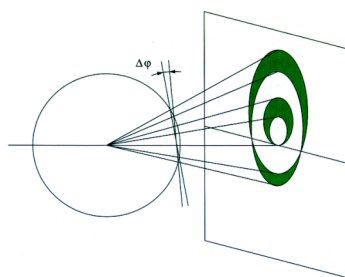
When reciprocal lattice points cross the Ewald sphere, their projections (from the centre of the Ewald sphere) appear as spots on the detector.

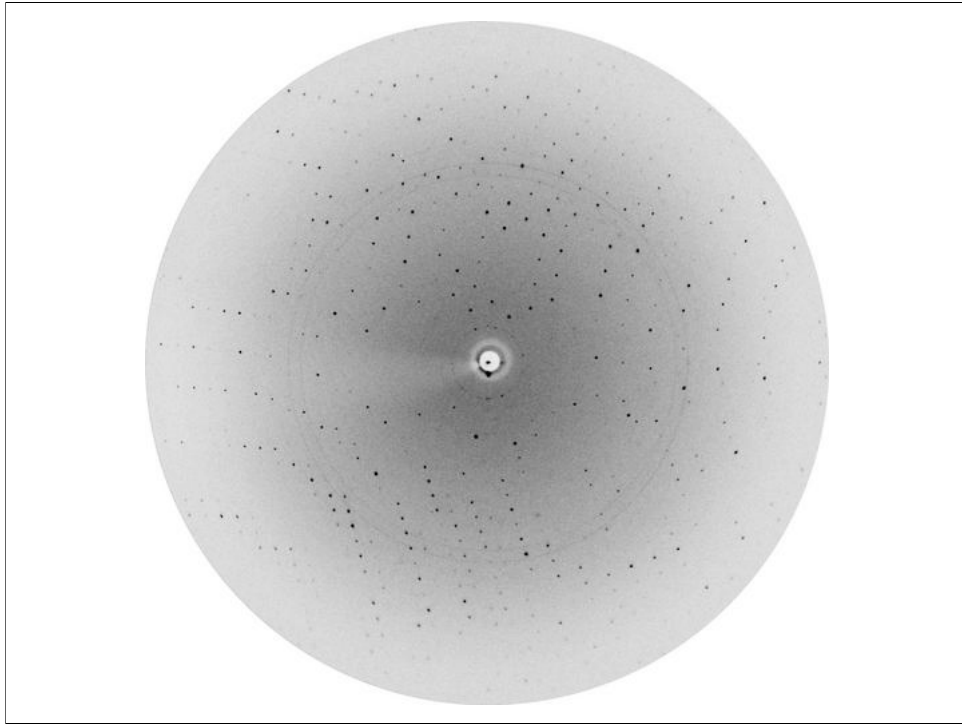
The appearance of diffraction images

Reciprocal lattice points lie in layers (planes). Each plane intersects the sphere in a circle, and the spots projected on the detector lie in ellipses



If the crystal is rotated through a small angle, each circle is broadened into a *lune*. All the spots in a lune belong to one plane of the reciprocal lattice (not necessarily a principal plane)





This movie is available at

<http://www.mrc-lmb.cam.ac.uk/harry/lmbtalk/camillo.mov>

The size of spots in reciprocal space and on the detector

Real observed diffraction is complicated by the imperfections of real crystals and X-ray beams

The X-ray beam

- the incident beam has a finite width and is not exactly parallel (*beam divergence*)
- the beam is not entirely monochromatic (*dispersion*)

The crystal

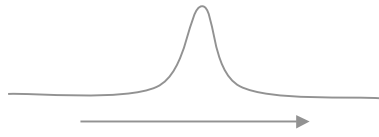
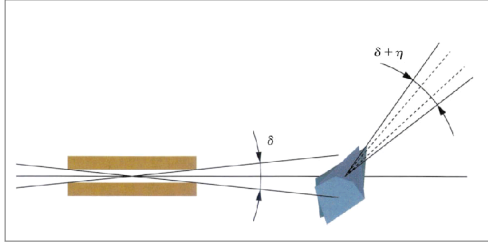
- the crystal has a finite size
- the crystal is not perfect, but may be considered a mosaic of blocks in slightly different orientations (*mosaicity*)

The effect of these factors can be considered as a broadening of the reciprocal lattice points, giving them a non-zero size

The incident beam at synchrotrons usually has a different divergence in the horizontal and vertical planes. The divergence from laboratory sources may have different values in the two dimensions depending on the optics, but it can usually be thought of as isotropic.

There is no reason why mosaicity should be the same in each dimension except for crystals with cubic symmetry, but we normally model it as a single parameter which refines according to the orientation of the crystal with respect to the incident radiation.

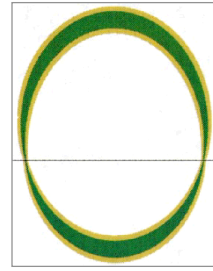
Beam divergence δ and mosaicity η add up to increase the angular width of the diffracted beam



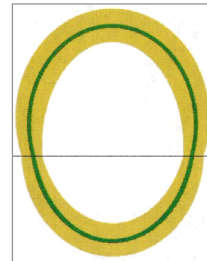
rotation angle ϕ

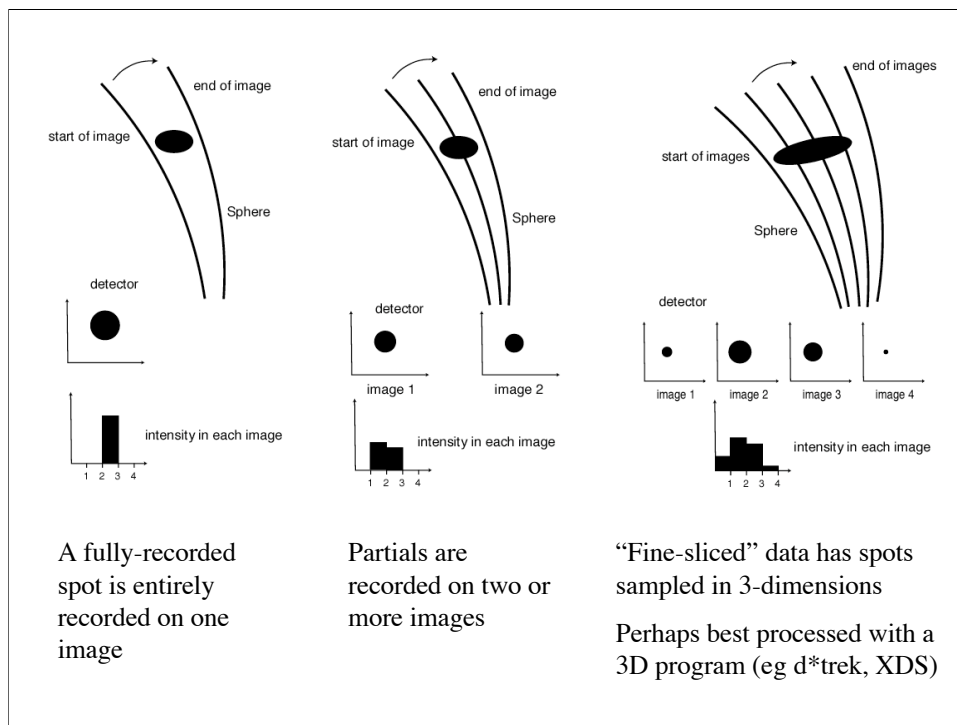
Reflection width in rotation
 $= \delta + \eta + \text{geometric factor}$

(geometric factor depends on angle between the rotation axis & \mathbf{S})



High mosaicity causes broadening of the lunes
 Most obvious along the rotation axis



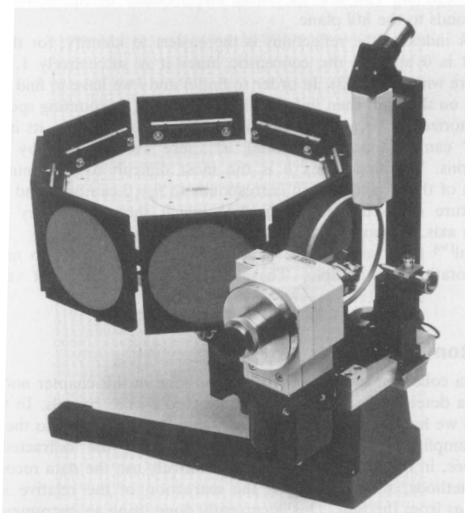


It is inevitable that fully-recorded spots will have “extra” background included in their diffraction intensity, since the background will be recorded during that part of the exposure when the spot is not in the diffracting condition. Partials, on the other hand, may or may not have this “extra” background - in the example on the right, the two central partials do not have the extra background but the first and last partials do.

If the readout time of a detector is slow, it is more efficient to collect fewer images in order to make up a complete dataset (fine slicing inevitably requires more images for the same total rotation range). This is why it is more normal for data collections using image plates to be coarse phi-sliced, but for those using CCDs to be fine-sliced.

Data Collection & Processing

Nearly all current single crystal data collection uses the screenless rotation method popularized by Uli Arndt and Alan Wonacott in the early 1970's.



A dataset is composed of successive images collected while rotating the crystal by a small angle (typically $0.1 - 2.0^\circ$) about a fixed axis - usually referred to as the ϕ axis, but when using multicircle diffractometers it is usually the ω axis. Since the Arndt-Wonacott oscillation camera was introduced, a number of solid state detectors have been developed to make the process somewhat easier and more automated.

Virtually all macromolecular (and small molecule) datasets are collected this way.

Auto-indexing

Indexing provides us with information about the crystal in its current setting:

- approximate cell dimensions
- putative crystal symmetry
- orientation with respect to diffractometer

Nearly always performed these days by auto-indexing, of which the most reliable method is based on the Fast Fourier Transform -

Mosflm, d*Trek, Labelit - one-dimensional FFT
Denzo (HKL) - three-dimensional FFT

These items are used as prior information in the integration step - they allow the placement of measurement boxes on diffraction spots.

Spots on an oscillation image are a distorted projection of the reciprocal lattice; provided the centres of the lattice points in the image lie *exactly* on the Ewald Sphere, we can calculate the scattering vector for each lattice point;

$$s = \begin{pmatrix} D/r - 1 \\ X_d/r \\ Y_d/r \end{pmatrix}$$

D = crystal to detector distance

X_d = X co-ordinate on image

Y_d = Y co-ordinate on image

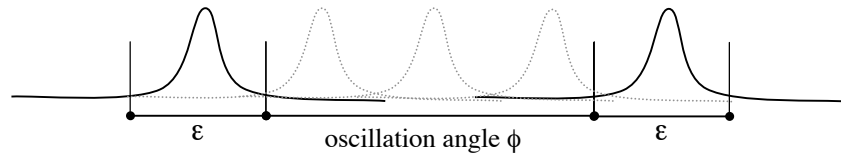
r = $(X_d^2 + Y_d^2 + D^2)^{1/2}$

These must be put onto a common frame with reference to the ϕ angle of each reflection

Since the spots have finite size and are broadened due to the effects already noted, and can appear on several adjacent images, we do need to have some caution when applying this model.

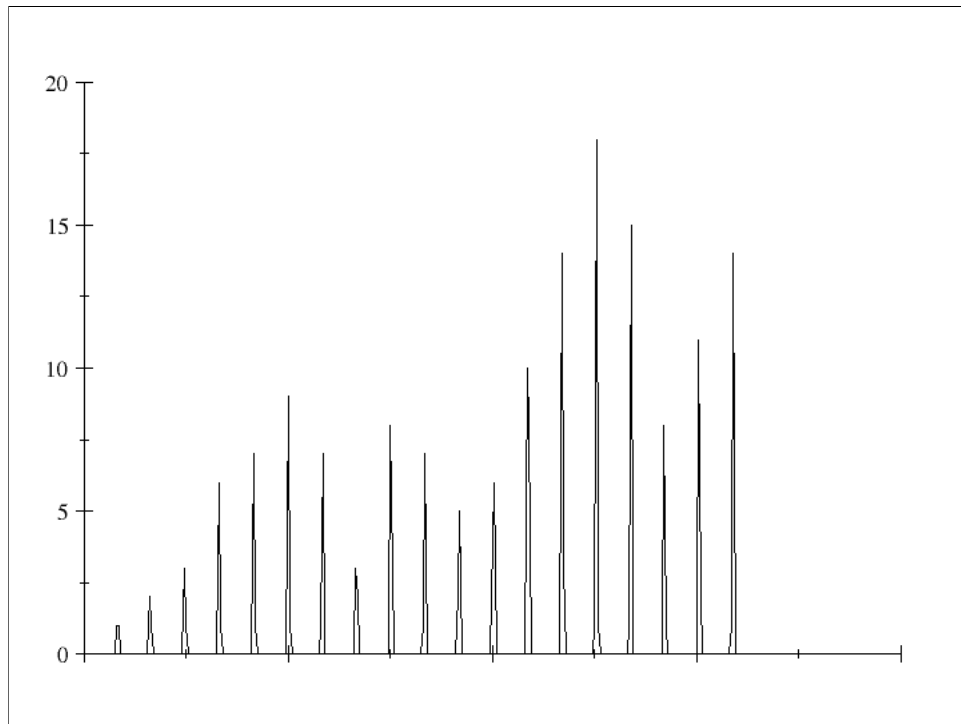
However, we don't know the ϕ angle of each reflection!

e.g. for an image with oscillation range $0.0^\circ - 1.0^\circ$, and a reflection with width ε° (in ϕ), we know that it lies in the range $-\varepsilon/2 : 1.0 + \varepsilon/2$.



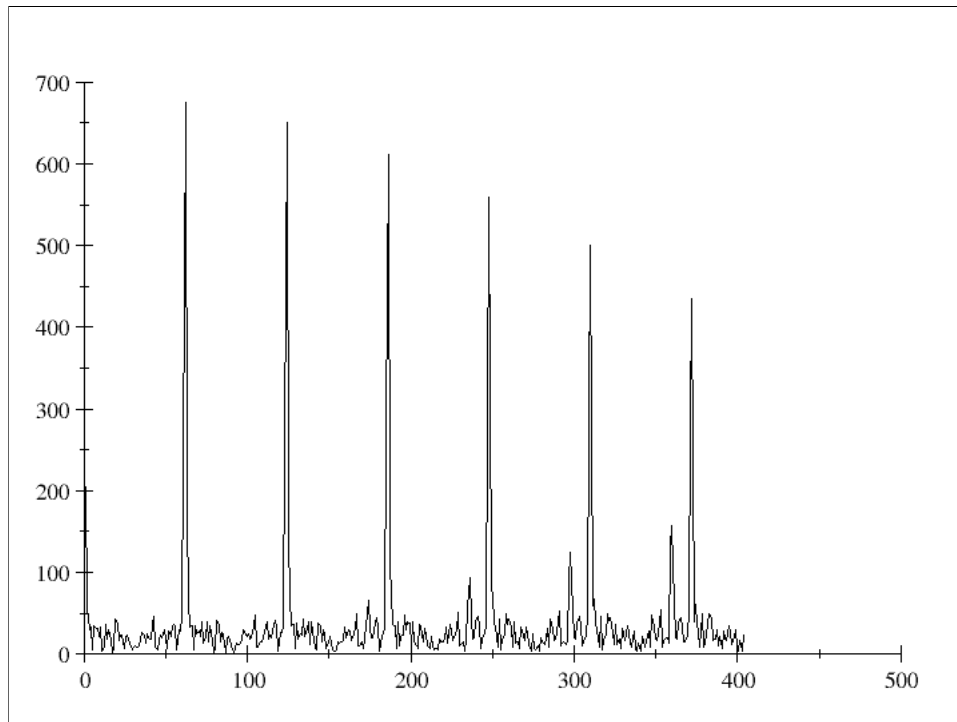
In general, both ε and ϕ are different for every reflection.

It is convenient to approximate ϕ to the mid-point of the image in question.



Thus the diffraction maxima (which fall on the lunes) can be mapped back (approximately) onto the reciprocal lattice. All spots within the same lune will give rise to a projected vector of the same length if mapped onto a zone axis (*i.e.* an axis corresponding to a crystal axis). Each cluster of scattering vectors will correspond to a vector between adjacent reciprocal lattice planes (*e.g.* $h=1, h=2, h=3, \text{etc.}$).

This is a real example of a 1D projection of the reciprocal lattice calculated from the ADSC Quantum 4 image used elsewhere in this talk. It corresponds to a real space axis of $\sim 62\text{\AA}$, but there is no way that you can tell this unless you also know the size of the “bins” for the projection in reciprocal space. The 1D FFT calculated from this projection is shown in the next slide.



Because of the regularity of these clusters, the Fourier transform will form a series of regularly spaced large maxima, where the distance between the maxima corresponds to the real-space axial length.

If the scattering vectors are mapped back onto a general vector which does not correspond to a zone axis, there is no clustering and the FFT does not have a regular array of maxima.

In practice, we calculate a total of ~ 3000 projections in small steps ($\sim 1 - 2^\circ$) around a complete hemisphere of directions, calculate FFTs for each, and pick those with (a) the largest maxima and (b) an appreciable interaxial angle.

3D methods use the 3D reconstruction of the reciprocal lattice and calculate a single 3D FFT - which takes $\sim 10^3 - 10^4$ times as long as each 1D FFT here, so relative speed is not an issue between the two methods.

Applying characteristic lattice symmetry

No	PENALTY	LATT	a	b	c	alpha	beta	gamma	Possible spacegroups
17	113	mC	85.58	85.65	58.56	89.9	133.3	87.0	C2
16	64	tI	62.10	58.93	85.46	89.7	85.4	90.0	I4,I41,I422,I4122
15	64	mC	101.51	58.93	62.10	90.0	122.9	89.7	C2
14	63	oI	58.56	62.33	85.65	85.8	89.9	90.1	I222,I212121
13	62	cF	85.58	85.46	85.65	93.1	87.0	93.6	F23,F432,F4132
12	61	hR	58.93	62.13	144.98	92.8	89.8	118.1	H3,H32 (hexagonal)
			58.82	58.56	62.10	61.9	61.8	62.0	R3,R32 (primitive)
11	61	mC	102.16	58.56	62.33	90.1	123.3	89.9	C2
10	57	oI	58.56	62.33	85.65	85.8	89.9	90.1	I222,I212121
9	56	mC	85.58	85.65	58.56	89.9	133.3	87.0	C2
8	55	mC	103.67	62.33	58.56	89.9	124.3	93.5	C2
7	10	mC	102.16	58.56	62.33	90.1	123.3	89.9	C2
6	8	mC	101.51	58.93	62.10	90.0	122.9	89.7	C2
5	7	hR	58.56	58.93	156.34	90.1	90.0	119.9	H3,H32 (hexagonal)
			62.10	62.13	62.33	56.5	56.4	56.4	R3,R32 (primitive)
4	5	mC	101.51	58.93	62.10	90.0	122.9	90.3	C2
3	2	mC	102.16	58.56	62.33	90.1	123.3	89.9	C2
2	0	aP	58.56	58.82	62.10	62.0	61.9	60.3	P1
1	0	aP	58.56	58.82	62.13	90.1	118.1	119.7	P1

The primitive triclinic cell found by autoindexing is transformed to each of the 44 characteristic lattices, and a penalty for each transformation is calculated according to a goodness of fit.

There is usually a sharp jump in the penalty from the worst good solution to the best bad solution (here the jump lies between solutions 7 and 8. Normally the best option is to choose the highest symmetry solution below the jump, since this is nearly always correct (in this case the rhombohedral solution, #5, would be chosen).

It is, however, important to remember that this is not necessarily the case - It is very important to remember that, while the metric symmetry usually indicates the correct lattice type, strictly speaking, the symmetry cannot be confirmed until a later stage of processing. Sometimes the unit cell indicates a higher symmetry than is actually present in the crystal; it is perfectly possible to have an orthorhombic cell with two axial lengths (a and b, for example) apparently equal.

Refinement of parameters

Successful integration of an image requires accurate crystal and detector parameters. Crystal and detector parameters can be refined by two complementary methods:

(1) Spot position on detector, minimize:

$$\Omega_1 = \sum_{i=1}^n w_{ix} (X_i^{calc} - X_i^{obs}) + w_{iy} (Y_i^{calc} - Y_i^{obs})$$

n.b. i) rotation of crystal about phi axis has no effect on this residual so it can't be refined.

ii) cell dimensions and other parameters (*e.g.* crystal to detector distance) may be strongly correlated.

Auto-indexing provides approximate crystal parameters which should be optimized before integrating the images so that the fit between observed and calculated spot positions is optimized and accurate cell parameters may be obtained (though it is possible to do this *a posteriori*).

Basically, there are 3 classes of parameters;

- (1) crystal (cell, orientation, mosaic spread)
- (2) detector (position, orientation, distortion)
- (3) beam (orientation, beam divergence).

Mosflm refines two residuals, in order to decouple the refinement of otherwise closely correlated parameters.

The spatial residual above is a simple method of refining crystal and instrument parameters, and has the advantage that no knowledge is required of the spot intensities - only their positions on the detector, as well as crystal to detector distance *etc.* It has a relatively wide radius of convergence, so is useful in the early stages of refinement (and is used in the autoindexing step of Mosflm for cell dimension and crystal orientation refinement).

Refinement of parameters

(2) Phi centroid method, minimize:

$$\Omega_2 = \sum_{i=1}^n w_i \left[\frac{(R_i^{calc} - R_i^{obs})}{d_i^*} \right]^2$$

n.b. (i) need a reasonable knowledge of intensities for this, so it can only be done after integration - hence *post-refinement*

(ii) need a model for the rocking curve

(iii) can refine either mosaicity or beam divergence.

However, if only low resolution data are being used in the refinement, there is a very strong correlation between cell parameters and crystal to detector distance; if high resolution reflections are included, this correlation becomes weaker. Also, if one axis is more or less parallel to the incident radiation, this axial length will be ill-defined and the refinement will not be reliable if performed with data from a single image.

This second method can only be used once intensities have been measured on at least two adjacent images. The reflections used cannot be fully recorded on a single image, as intensity information is required from all parts of partials spread over different images. The relative fractions of the images are used to produce a very accurate result, but the refinement has a relatively narrow radius of convergence, so it can only be used once reasonably accurate values have been determined.

Mosflm uses the spatial residual to refine the detector parameters, and post-refinement for the crystal and beam parameters. Since the mosaic spread and the beam divergence refinements are closely correlated, only one may be refined.

Integration

In its simplest form, this involves simply adding together the values of the pixels in each spot and subtracting the background counts under the spot.

Two distinct types:

2D - Mosflm, Denzo

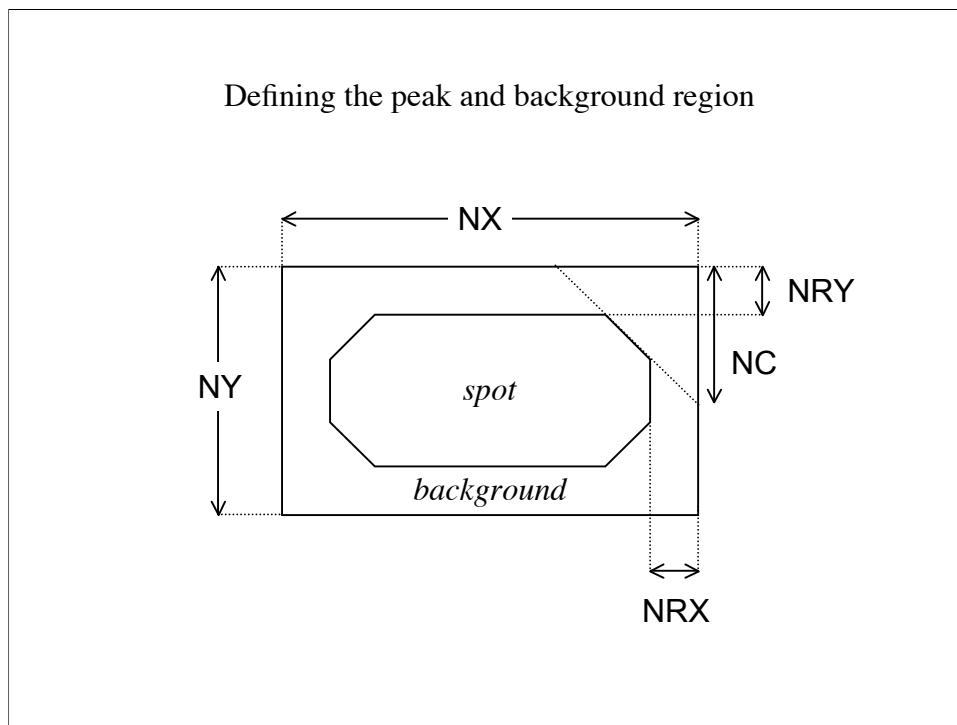
Partials are measured by profile fitting and are only summed during scaling and merging

3D - XDS, d*Trek

Partials are summed together by fitting to a reflection profile which extends into a third dimension (images adjacent in ϕ)

We recommend refining the cell dimensions prior to integration, then holding them fixed during the integration itself, provided there is no evidence of gross radiation damage to the crystal during data collection. The principal reason for this is that it is likely that in at least one orientation a zone axis will be more-or-less parallel with the X-ray vector, so only limited information regarding that cell length will be available in that orientation and the refinement consequently unstable.

In integration, counting statistics allow us to calculate an error estimate of the intensity (the “sigma” or ESD).



All common programs use a mask to define the spot area itself and a background region surrounding this. The background is used to estimate the unmeasurable background under the spot itself. Some programs also use a “guard” region between the spot and background, but this has been found to have no significant effect on measurement.

Typically, the background region is $\sim 3x$ the size of the spot region in order to give good statistics to its measurement.

The mask in Mosflm is automatically determined and optimized if it is not supplied by the user.

(1) Summation integration

(a) Integration in the absence of X-ray background or detector noise

Assign each pixel to the nearest reciprocal lattice point. Sum all pixels to obtain the integrated intensity.

There is no penalty (in $I/\sigma I$) for including pixels beyond the physical extent of the diffraction spot.

This situation is never realized in practice, even for very strong spots.

Summation integration is fast and simple. The values of pixels within the calculated boundaries of the diffraction spot are simply added together to give the intensity of the spot. There may be cases when it is more appropriate than profile fitting the reflections.

It is also called the “box-sum” method.

(2) Integration by Profile Fitting

Summation integration is unbiased (providing peak and background regions are correctly defined) but gives poor signal to noise ($I/\sigma I$) for weak reflections. Profile fitting can improve the estimation of weak intensities.

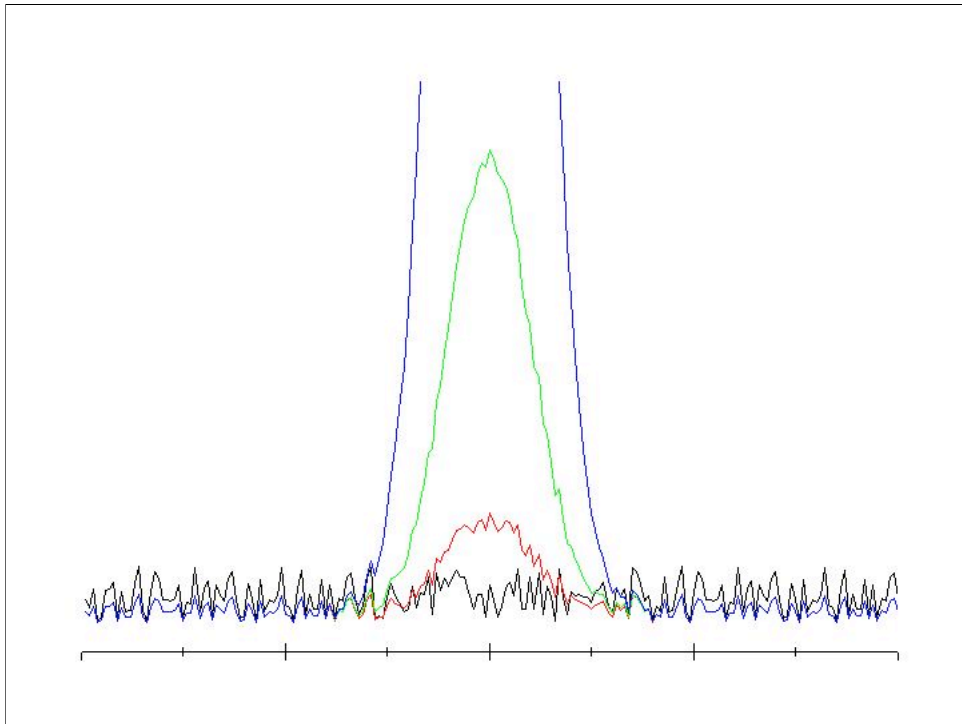
$$R = \sum_{i=1}^{\text{peak pixels}} w_i [X_i - KP_i]^2$$

↑
scale factor

Profile fitting is based on the premise that reflections on nearby parts of the detector have essentially the same shape on the detector in two dimensions and differ only in height or intensity. The same profile, stretched “up” or squashed “down” should fit all reflections (provided that the variation across the surface of the detector is taken into account); an analytical profile can be calculated and the best fit refined against a large sample of reflections. The intensity of each reflection is calculated by determining the scale factor which gives the best fit of its observed box-sum intensity to the profile.

The next slide, illustrates that the *apparent* width of reflections is less for weak spots than for stronger. Each of the “reflections” above was calculated with the same width and background noise levels - the only difference is the intensity in each case.

In practice, profiles based on both fully recorded and partially recorded reflections give very similar data quality to those based on fully recorded reflections only.



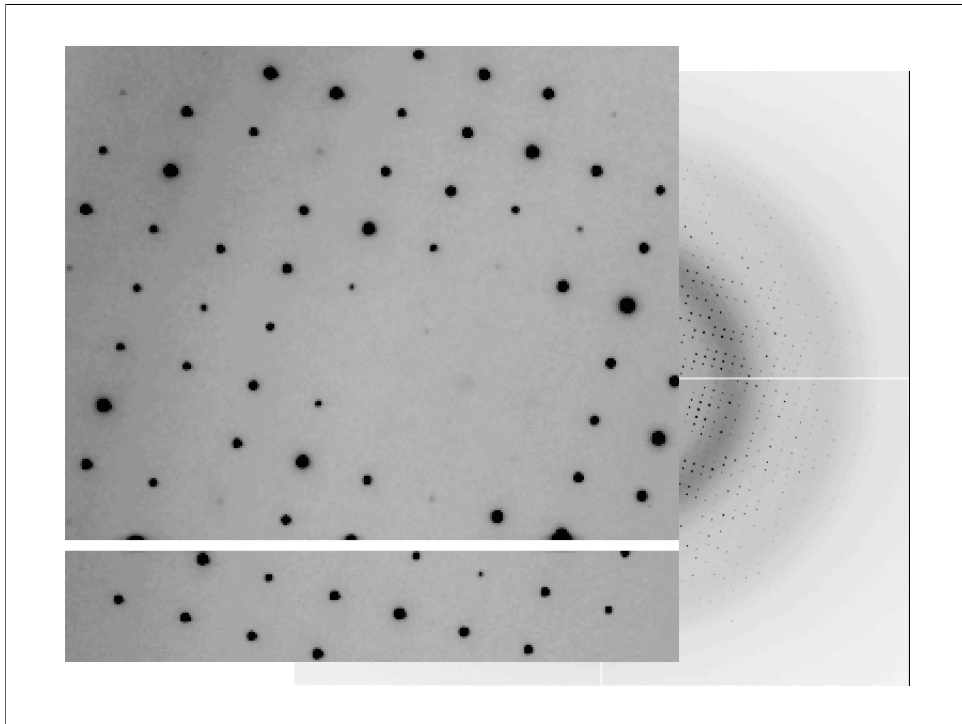
Variations in spot shape across the face of the detector need to be allowed for. This can be done in two ways;

(1) different profiles need to be evaluated for different regions of the detector, and a weighted sum of these standards used for evaluating each reflection (*MOSFLM*). The standard profiles are usually accumulated over many images (10-20, determined by the “BLOCK” subkeyword) so that most partials will be summed to give the equivalent fully recorded spot profile.

(2) a separate profile is evaluated for each reflection using other reflections within a specified distance of the reflection being integrated (*DENZO*, "profile fitting radius").

It is important to remember that the spot intensity does not affect the width of the reflections. In this real example, the weak reflections are apparently narrower than the strong, but this is only because their shoulders are hidden beneath the background noise.

Partial reflections, on the other hand, are often narrower than fulls. This is simply because the reflections have a finite volume, and if only part of this volume has swept through the Ewald sphere, it has a smaller size than the whole.



Problems with profile fitting

(1) Profile fitting small, strong spots can be problematic. A small error in the profile can be magnified and give rise to systematic errors in very strong reflections since the errors themselves are proportional to the intensity of the peak, and are the major determining factor in the measurement of the peak.

(2) There is an artificial broadening of the peak associated with the formation of the standard profiles; this is more serious for small spots than for large.

(3) If the spot shape really does vary across the detector (perhaps due to a split or bent crystal), the profile used may not be valid.

(1) and (2) may be dealt with by merging and scaling profile fitted intensities for weak reflections, and summation intensity measurements for strong reflections. Both measurements are stored by Mosfilm and Scala allows this process to be performed.